

Anandamide Activates Vanilloid Receptor 1 (VR1) at Acidic pH in Dorsal Root Ganglia Neurons and Cells Ectopically Expressing VR1*

Received for publication, February 20, 2001, and April 26, 2001
Published, JBC Papers in Press, May 1, 2001, DOI 10.1074/jbc.M101607200

Zoltan Olah‡, Laszlo Karai, and Michael J. Iadarola

From the Neuronal Gene Expression Unit, Pain and Neurosensory Mechanisms Branch, NIDCR, National Institutes of Health, Bethesda, Maryland 20892

The vanilloid receptor type 1 (VR1) is a heat-activated ionophore preferentially expressed in nociceptive neurons of trigeminal and dorsal root ganglia (DRG). VR1, which binds and is activated by capsaicin and other vanilloid compounds, was noted to interact with the endocannabinoid anandamide (ANA) and certain inflammatory metabolites of arachidonic acid in a pH-dependent manner. At pH ≤ 6.5 ANA induced $^{45}\text{Ca}^{2+}$ uptake either in primary cultures of DRG neurons or cells ectopically expressing C-terminally tagged recombinant forms of VR1 with an $\text{EC}_{50} = \sim 10 \mu\text{M}$ at pH 5.5. Capsazepine, a potent antagonist of vanilloids, inhibited ANA-induced Ca^{2+} transport in both cell systems. Vanilloids displaced [^3H]ANA in VR1-expressing cells, suggesting competition for binding to VR1. Ratiometric determination of intracellular free calcium and confocal imaging of the VR1-green fluorescent fusion protein revealed that, at low pH (≤ 6.5), ANA could induce an elevation of intracellular free Ca^{2+} and consequent intracellular membrane changes in DRG neurons or transfected cells expressing VR1. These actions of ANA were similar to the effects determined previously for vanilloids. The ligand-induced changes in Ca^{2+} at pH ≤ 6.5 are consistent with the idea that ANA and other eicosanoids act as endogenous ligands of VR1 in a conditional fashion *in vivo*. The pH dependence suggests that tissue acidification in inflammation, ischemia, or traumatic injury can sensitize VR1 to eicosanoids and transduce pain from the periphery.

C-fiber nociceptors are thin unmyelinated processes present throughout the body that respond to noxious stimuli including heat, tissue injury, acidification, and inflammation. Platelets, leukocytes, spinal cord astrocytes, and other cell types respond to tissue injury with eicosanoid release (1–3). A linkage between generation of eicosanoids and pain sensation has been proposed; however, the range of mechanisms has not been fully determined (4). A high proton (H^+) concentration often coincides with inflammation, ischemia, and cancer growth (5, 6). It is hypothesized that acidification and eicosanoid release during inflammation may synergize to produce nociceptor sensitization, but the molecular mechanisms require elucidation.

The recently identified vanilloid receptor/ionophore (VR1),¹

expressed in DRG and trigeminal ganglion neurons, is capable of integrating physical and chemical stimuli at the molecular level (7, 8). Both noxious heat and vanilloid treatment evoke action potentials in primary sensory nociceptive neurons, and these effects are enhanced at a pH of less than 6.5 (8–11). An acidic extracellular milieu increases the number of channels available to be opened by capsaicin (12). However, H^+ alone (*i.e.* pH 5.0–6.0) does not activate VR1 in cultured DRG neurons (13).

Chemodenervation with capsaicin has demonstrated that the majority of epidermal “C” type axons belong to the capsaicin/vanilloid-sensitive population of sensory neurons (14). Capsazepine (CPZ), a well known antagonist of vanilloids, reduces hyperalgesic responses to inflammation, indicating that endogenous, vanilloid-like substances may be inhibited from acting *via* VR1 (15). Although these nerve endings respond to capsaicin and other plant-derived vanilloids (16), the endogenous pain signaling analog(s) of capsaicin have not been fully identified nor has their potential for toxicity been evaluated.

Recently, the endocannabinoid, anandamide (ANA), an analog of both eicosanoids and vanilloids, was shown to evoke inward current and depolarization in cells expressing recombinant VR1 (17). Other arachidonic acid metabolites or analogs such as PGE_2 and arvanil, which are distant homologs of vanilloids, also are active on both their cognate receptors as well as on VR1 (18, 19). The structural similarity of eicosanoids and vanilloids suggest that ANA and other metabolites of the lipoxygenase and cyclooxygenase pathways can “cross-talk” with VR1 under certain conditions. Although 12- and 15-(*S*)-hydroperoxyeicosatetraenoic acids, 5- and 15-(*S*)-hydroxyeicosatetraenoic acids, and leukotriene B (4) are currently reported to activate recombinant VR1 (4), only a few eicosanoids, including prostaglandin, prostacyclin and PGE_2 , are reported to be proalgesic (20, 21).

In contrast to the potential pro-algesic actions outlined above, ANA is much better known as an analgesic agent in persistent pain models through actions on the cannabinoid receptors, CB1 and CB2 (22, 23). SR 141716A, a CB1-selective antagonist, reverses the behavioral effects of anandamide-treated rats, whereas other agonists are anti-allodynic in rats with persistent inflammation (24–26). In contrast to the analgesic actions of cannabinoids, little is known about the pain-related effects of endocannabinoids. ANA-induced Ca^{2+} transport has recently been revealed in cells expressing recombinant human VR1 but not verified by Ca^{2+} uptake experiments on nociceptive neurons (27–29), and the physiological relevance of ANA-VR1 interaction continues to be debated (30, 31).

Dulbecco’s modified Eagle’s medium; 12(*S*)HPETE, 12-(*S*)-hydroperoxyeicos-5Z,8Z,10E,14Z-tetraenoic acid; 12(*S*)HETE, hydroxyeicos-5Z,8Z,10E,14Z-tetraenoic acid; PG, prostaglandin; ANA, anandamide; MES, 2-(*N*-morpholino)ethanesulfonic acid.

* The costs of publication of this article were defrayed in part by the payment of page charges. This article must therefore be hereby marked “advertisement” in accordance with 18 U.S.C. Section 1734 solely to indicate this fact.

‡ To whom correspondence should be addressed: Bldg. 49, Rm. 1A19, NIH, 49 Convent Dr., MSC-4410, Bethesda, MD 20892-4410. Tel.: 301-496-2755; Fax: 301-402-0667; E-mail: zoltan.olah@nih.gov.

¹ The abbreviations used are: VR1, vanilloid receptor type 1; CAP, capsaicin; CPZ, capsazepine; OLV, olvanil; RTX, resiniferatoxin; DRG, dorsal root ganglion; ER, endoplasmic reticulum; VR1e, C-terminally e-tagged vanilloid receptor; eGFP, enhanced green fluorescent protein; VR1eGFP, VR1-enhanced green fluorescent fusion protein; DMEM,

It can be hypothesized that eicosanoids need other inflammatory factors, such as tissue acidification for their action on VR1. Thus, conditionally released or otherwise weak endogenous ligands at neutral pH can be potentiated by protonation of VR1. To study the potential role of arachidonic acid metabolites in pain signaling, assays were carried out on cultured DRG neurons and cells expressing C-terminally tagged recombinant versions of VR1. We used two methods to examine ligand-induced VR1 ionophore activity: $^{45}\text{Ca}^{2+}$ uptake from the media and changes in $[\text{Ca}^{2+}]_i$ determined with calcium-sensitive fluorescent dye labeling and ratiometric confocal microscopy. Two rat VR1 expression constructs were examined. The first was a short, ϵ -epitope-tagged VR1 recombinant (VR1 ϵ) stably expressed in NIH 3T3 cells under the control of a weak cellular promoter. The second construct, a VR1-enhanced green fluorescent fusion protein (VR1eGFP), was used for the real time imaging of the dynamics of agonist-induced intracellular membrane remodeling *in vivo*. We have shown previously that membrane remodeling that involves ER (32–35) and mitochondrial vesiculation (35) provides robust end points to assess agonist-driven Ca^{2+} ionophore activity (35).

Confocal microscopy of vanilloid- or ANA-treated live DRG neurons and VR1eGFP-expressing cells disclosed an elevation of $[\text{Ca}^{2+}]_i$, followed by fragmentation of the ER and mitochondria. The eicosanoid-induced Ca^{2+} toxicity can result in intracellular dysfunction and axonal damage of VR1-positive DRG neurons. If the cell bodies of nociceptors are exposed to ANA or inflammatory eicosanoids, cell death may ensue through toxic accumulation of $[\text{Ca}^{2+}]_i$. Our data suggest that low pH acts as a switch to convert VR1 to a form that binds ANA and eicosanoids. Thus, at low pH ANA and eicosanoids can have algescic or pro-algescic effects via VR1 at nociceptive endings as well as contribute to potential neuropathological processes in the peripheral nerve or sensory ganglia.

EXPERIMENTAL PROCEDURES

Recombinant Materials—C-terminally tagged chimeric rat VR1eGFP and VR1 ϵ were prepared in the pEGFP-N3 (CLONTECH) and pMTH (36) plasmid vectors, respectively, as described (35). The plasmid constructs were transiently transfected in COS7, HEK293, and NIH 3T3 cells, and the expressed chimeric VR1 proteins were extensively characterized using biochemical and electrophysiological assays and fluorescence confocal microscopy (35).

Transient Transfection—HEK 293 and COS7 cells (10^5) were plated on 25-mm glass slides for live cell confocal microscopy or seeded in 24-well plates for calcium transport experiments 1 day before transfection. GenePorter purchased from Gene Therapy Systems (San Diego, CA) was used as the transfection reagent. Transfections were carried out according to the recommendations of the manufacturer. For the 25-mm slides 3 μg and for the 24-well plates 2 μg of DNA/well were used together with 25 and 10 μl of GenePorter reagent, respectively. The DNA and the GenePorter were mixed in serum free Opti-MEM (Life Technologies, Inc.) for 15 min at room temperature then placed on the cultured cells. After 3 h at 34 °C the incubation medium was supplemented with an equal volume of complete Dulbecco's modified Eagle's medium (DMEM) containing 10% fetal bovine serum, 1% streptomycin, and 1% glutamine. To prevent acidification of the culture medium, the pH was buffered to 7.4 with 20 mM HEPES. To diminish heat-induced activation of VR1, cells were cultured in an incubator adjusted to 34 °C. Transiently transfected cells with green VR1eGFP fluorescence were counted on an inverted fluorescence microscope or quantified in a microplate fluorimeter at 515 nm, employing the 488 nm absorption band of eGFP.

Preparation of VR1 ϵ -expressing NIH 3T3 Cell Line—To develop cell lines permanently expressing VR1 ϵ , we used NIH 3T3 cells, which we determined to have a low endogenous level of Ca^{2+} transport that was not inducible with vanilloids or ANA. To avoid toxicity that occurs with VR1 overexpression, VR1 ϵ was expressed using only the basal activity of the metallothionein (pMTH) promoter. The C-terminal 12-amino acid ϵ -epitope allowed immunological detection and verification of ectopic expression. To prepare a cell line permanently expressing VR1 ϵ , NIH 3T3 cells were transiently transfected with the pMTH-VR1 ϵ plasmid.

After 24 h cells were transferred into 24-well plates and incubated with complete DMEM and selection medium, containing 0.8 mg/ml geneticin (G418) buffered with 20 mM HEPES (pH 7.4) to stabilize the pH. Cell lines expressing VR1 ϵ were selected at 34 °C. In addition, to minimize heat-induced VR1 channel activation and Ca^{2+} cytotoxicity, the selection medium was changed every second day. After 1 month G418-resistant colonies were tested with vanilloid-induced Ca^{2+} transport assays. A colony exhibiting RTX-induced $^{45}\text{Ca}^{2+}$ uptake 20-fold above the base line determined in comparison with parental NIH3T3 cells was chosen for further studies.

DRG Culture—DRG neuron-enriched cultures were prepared from embryonic rats (embryonic day 16) (35). Briefly, DRGs were dissected and then processed in fresh dissection medium (Lebowitz medium; Life Technologies, Inc.) until plated in DMEM. The DMEM contained 20 mM HEPES (to prevent acidification and stabilize pH at 7.4), 7.5% fetal bovine serum, 7.5% horse serum, 5 mg/ml uridine supplemented with 2 mg/ml 5-fluoro-2'-deoxyuridine, and 40 ng/ml nerve growth factor to inhibit cell division and to promote differentiation of long neuronal processes, respectively. Cells were seeded on 25-mm glass coverslips or on multi-well microtiter plates. Surfaces were coated with poly-D-lysine and laminin. The cultures were selected in this medium for 1 week, at which point well differentiated neurons and nondividing cells dominated the population. Primary DRG cultures in this stage were used in Ca^{2+} transport assays and confocal microscopy.

Ca^{2+} Transport— $^{45}\text{Ca}^{2+}$ uptake experiments were carried out on the primary DRG cultures (10^4 cells/well) after 1 week of neuronal growth factor and 5-fluoro-2'-deoxyuridine treatment and on transiently transfected HEK293 cells (10^5 /well) expressing VR1eGFP for at least 36–48 h. For comparison, $^{45}\text{Ca}^{2+}$ transport assays were performed on NIH 3T3 cells permanently expressing the ϵ -tagged VR1 under control of the basal activity of the metallothionein promoter.

The cells were washed once in Hanks' balanced salt solution (pH 6.0) supplemented with 10 μM Ca^{2+} and 0.1 mg/ml bovine serum albumin (HCB) and adapted to room temperature (24 °C) for 5 min. $^{45}\text{Ca}^{2+}$ uptake was performed for 10 min at 24 °C in HCB using 0.2 μCi of $^{45}\text{Ca}^{2+}$ as radioactive tracer in a 200- μl final volume. To determine the pH dependence of the $^{45}\text{Ca}^{2+}$ uptake, HCB was buffered with 20 mM Tris-HCl, adjusted to the indicated pH with 1 M MES (HCBTM). Anandamide was prepared in a Soya oil/water (1:4) emulsion. RTX and CAP were diluted at least 10,000-fold from 10 mM ethanol stock solutions to the indicated final concentrations. To stop $^{45}\text{Ca}^{2+}$ uptake, cells were rapidly changed back into 1 ml of HCB, washed two additional times with 1 ml HCB, and then lysed in 200 μl /well RIPA buffer (50 mM Tris-HCl, pH 7.5, 150 mM NaCl, 1% Triton X-100, 0.5% deoxycholate, 0.1% SDS, 5 mM EDTA) for 30 min. Aliquots of the solubilized cell extracts were counted in a liquid scintillation counter.

$[\text{H}]\text{ANA}$ Binding—Transfected HEK293 cells (10^5 /well) expressing VR1eGFP for 48 h were washed once in Ca^{2+} -free Hanks' balanced salt solution (pH 6.0) supplemented with 0.1 mg/ml bovine serum albumin (HB). Binding experiments were performed for 40 min at 4 °C in HB, except as radioactive tracer 0.5 μCi of $[\text{H}]\text{ANA}$ /ml was added in 500 μl incubation volume. To stop the binding, cells were rapidly changed back into 1 ml of ice-cold HB and washed rapidly two additional times with HB at 4 °C. The cells were lysed and processed for scintillation counting as described for $^{45}\text{Ca}^{2+}$ uptake.

Confocal Microscopy—An inverted Nikon microscope equipped with the 1024 MRC Bio-Rad laser confocal system was used for fluorescence studies. For ratiometric determination of cytosolic $[\text{Ca}^{2+}]_i$, DRG cultures were preloaded with 5 μM Indo-1 AM dye. After incubation for 30 min at 34 °C, the cells were washed three times in HCB to remove excess dye and kept in the dark for at least 15 min before starting the experiments. The recordings were carried out in 1 ml of HCB. The ratio of emitted fluorescence intensity at 405 and 485 was calculated from images taken at 10-s intervals. Following of recording of the base line, the drug was added in 100 μl of HCB.

To monitor the consequence of drug treatments and the effect of Ca^{2+} on intracellular membranes, cells were transfected with VR1eGFP. After 1 day and just before microscopy they were loaded with 0.5 μM MitoTracker dye as recommended by the manufacturer (Molecular Probes). Mitochondria and VR1eGFP were observed in live cells by dual fluorescence confocal microscopy employing appropriate filter sets to separate green (VR1eGFP) and red (MitoTracker) epifluorescence. To facilitate drug treatment, the experiments were performed in an open chamber system.

Western Blotting—Total protein extracts were prepared in denaturing SDS buffer and analyzed for immunoreactivity by Western blotting as described previously (36). VR1-specific antibody was raised in rabbits immunized with the N-terminal MEQRASLDSESESPPE peptide.

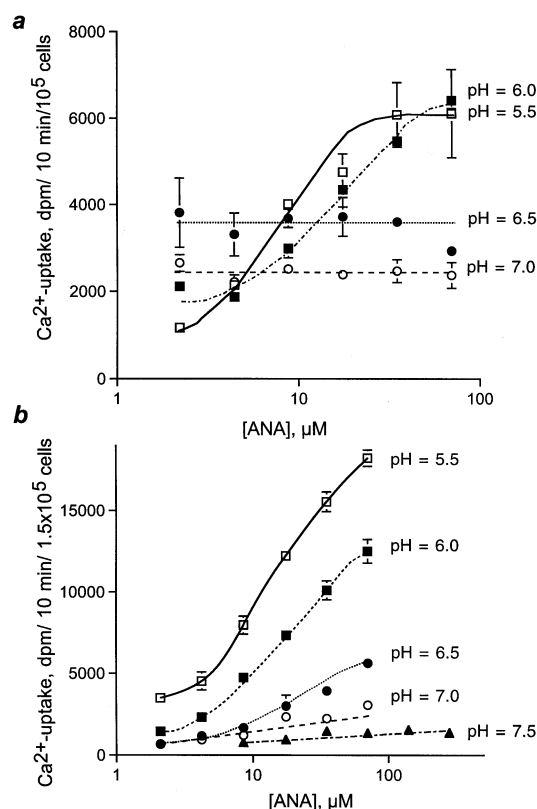


FIG. 1. Combined effect of pH and anandamide on dissociated DRG cultures (a) and cells stably expressing recombinant VR1ε (b). DRG cultures prepared from embryonic day 16 rat embryos were cultured for 1 week prior to assay. ANA at pH \leq 6.0 markedly induces $^{45}Ca^{2+}$ uptake in rat DRG cultures. In NIH 3T3 cells stably expressing VR1ε, ANA is effective at pH \leq 7.0. Cells were washed once in Hanks' balanced salt solution (pH 6.0) supplemented with 10 μ M Ca^{2+} and 0.1 mg/ml bovine serum albumin. The pH levels of the $^{45}Ca^{2+}$ uptake medium was adjusted with 20 mM Tris-MES buffer as indicated. $^{45}Ca^{2+}$ uptake assays were performed for 10 min at 24 °C. The aliquots of solubilized cell extracts were counted in a liquid scintillation counter. Each point on the graph is the average of triplicate determinations. The experiments were repeated at least two additional times in triplicate with similar results.

tide of rat VR1 conjugated to keyhole limpet hemocyanin. Antigen affinity-purified antibody was diluted 1000-fold for Western blot and immunocytochemistry experiments. This antibody preparation recognizes native rat VR1, as illustrated in Fig. 8, and chimeric VR1eGFP (35). Stripping of nitrocellulose blotting filters (Bio-Rad) was carried out in 200 ml of 50 mM Tris-HCl buffer (pH 7.5) containing 2% SDS and 0.1 M β -mercaptoethanol at 65 °C for 1 h. To demonstrate the eGFP portion of VR1eGFP, blots were incubated either with GFP specific rabbit antiserum (CLONTECH) and then with a cytochrome *c*-specific monoclonal antibody as suggested by the manufacturer (PharMingen International) to assess equality of protein loading and transfer. Enhanced chemiluminescence was used to visualize primary antibody binding according to the manufacturer's protocol (New England Biolabs).

Materials—ANA (1:4 soy bean oil:water emulsion), olvanil (OLV) and RTX were purchased from Tocris. ANA in ethanol, 12(S)HPETE, 12(S)HETE, PGE₂, and PGD₂ were from Biomol, and CPZ and CAP were obtained from Calbiochem. ^{45}Ca was from ICN, and [3H]ANA was purchased from ARC.

RESULTS

Concentration-response curves from rat DRG cultures indicated that acidic pH markedly enhanced the actions of ANA on Ca^{2+} uptake (Fig. 1a). At pH 5.5 and 6.0 the EC₅₀ values of ANA-induced Ca^{2+} transport were determined from Hill plots fitted to the data to be 7 and 10 μ M, respectively. At pH \geq 6.5, Ca^{2+} uptake in DRG cells did not increase with increasing ANA concentrations, although the base-line Ca^{2+} uptake was higher at pH 6.5 than at pH 7.0. Application of the highest concentra-

tion of vehicle (1:10 dilution of the 1:4 soy oil:water emulsion stock) was without effect on cultured DRG neurons (not shown). The observed effect of ANA was specific to primary nociceptive neurons. No similar pH-dependent, ANA-induced Ca^{2+} uptake was found in embryonic rat spinal cord cultures. In fact, in spinal cord cultures a decrease in pH alone (*i.e.* pH 5.5) inhibited the short term (10 min) Ca^{2+} uptake. Furthermore, treatment of spinal cord cultures with the same amounts of ANA did not induce Ca^{2+} transport (not shown).

In NIH 3T3 cells stably expressing VR1ε, Ca^{2+} uptake assays were carried out at similar pH and ANA concentrations. As with the DRG neurons, ANA treatment at progressively lower pH produced progressively more Ca^{2+} uptake (Fig. 1b). The EC₅₀ values of ANA were comparable with those of the DRG neurons: 14 \pm 5, 25 \pm 5, and 63 \pm 12 μ M, at pH 5.5, 6.0, and 6.5, respectively, indicating an increasing affinity of VR1 toward ANA at lower pH. At pH \geq 7.0 little or no effect was found with increasing ANA concentration (Fig. 1b). In the parental NIH 3T3 cell line, in repeated experiments, H^+ , ANA, and the vehicle (soy oil:water (1:4) emulsion at a 1:10 dilution) had no effect on basal Ca^{2+} uptake (not shown). The vehicle also did not affect Ca^{2+} uptake in NIH 3T3 cells expressing VR1ε.

We next compare at pH 6.0, under mildly acidic conditions, the efficacy of ANA to RTX and CAP, which are known vanilloid agonists. In primary DRG cultures nanomolar RTX or 0.5 μ M CAP induced \sim 15–20-fold elevation over the basal Ca^{2+} uptake. Under the same experimental conditions, ANA was effective in the 10–100 μ M range, increasing the influx levels more than 3-fold over basal Ca^{2+} uptake (Fig. 2a). The induction of Ca^{2+} uptake by 0.01 μ M RTX, 1 μ M CAP, and 100 μ M ANA was almost completely inhibited by 10 μ M CPZ, a VR1 antagonist (Fig. 2a). Treatment with maximal amounts of vanilloid vehicle (*i.e.* final concentration of 0.05% EtOH added with CAP and CPZ) was without effect on the cultured DRG neurons (not shown).

The results determined in DRG cultures were compared with VR1-mediated Ca^{2+} uptake in cells transiently expressing VR1eGFP (35). The expression levels of VR1eGFP can be estimated *in situ* by fluorescence microscopy, which showed that VR1eGFP-transfected cells represented \sim 30% of the population. In Fig. 2b $^{45}Ca^{2+}$ uptake experiments in HEK293 cells transiently expressing VR1eGFP are shown. These cultures were treated with increasing concentrations of CAP, RTX, and ANA during the 10-min period of the $^{45}Ca^{2+}$ uptake assay. The uptake kinetics of the transfected HEK293 cells were similar to those determined in primary DRG culture (Fig. 2a). In both cultures, vanilloids increased the $^{45}Ca^{2+}$ uptake more than 10-fold over base line in nanomolar to micromolar concentrations. In comparison, ANA was somewhat more effective in DRG neurons. At pH 6.0 ANA stimulated $^{45}Ca^{2+}$ uptake about 5–10-fold in the 10–100 μ M concentration range. The EC₅₀ determined for RTX, CAP, and ANA were about 1.0, 200, and 30,000 nM, respectively (Fig. 2b). Similar results were obtained with transiently transfected COS7 cells expressing VR1eGFP (not shown). Nontransfected HEK293 or COS7 cells did not show any increase in $^{45}Ca^{2+}$ uptake in response to these compounds. In the absence of drug treatment, expression of VR1eGFP in different cell lines usually doubled the basal $^{45}Ca^{2+}$ uptake, an effect most likely caused by spontaneous channel activity of VR1 (data not shown).

H^+ dependence of RTX- and ANA-induced Ca^{2+} uptake was studied in side-by-side experiments (Fig. 3) using the NIH 3T3 cell line stably expressing VR1ε. Ca^{2+} uptake assays were carried out in buffered HCBTM in which the pH was adjusted between 7.5 and 5.5 with 1 M MES, as described under "Exper-

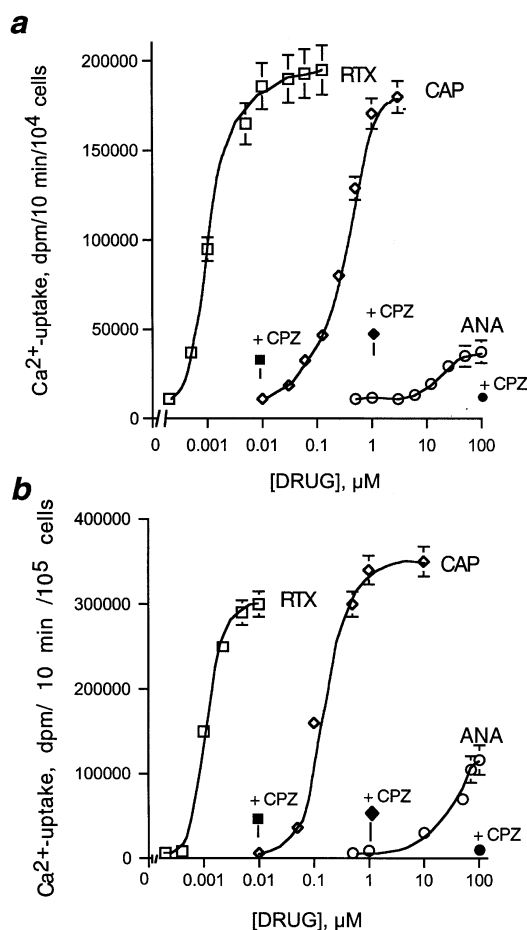


FIG. 2. RTX, CAP, and ANA induce Ca^{2+} uptake in a dose-dependent manner in DRG neurons (a) and in HEK293 ectopically expressing recombinant VR1eGFP (b). The HEK293 cells were transiently transfected with 2 μ g of VR1eGFP plasmid/well in 24-well plates 1 day before the Ca^{2+} uptake experiments. To demonstrate VR1 specificity, 10 μ M capsazepine, a vanilloid antagonist, was added simultaneously with the indicated concentrations of ligands (filled symbols). Capsazepine in this concentration almost completely blocked the VR1-specific responses, determined with co-incubation with 10 nM RTX, 1 μ M CAP, and 100 μ M ANA in both DRG cultures and HEK293 expressing VR1eGFP. Each point represents the mean \pm S.E. of triplicate determinations. Similar results were obtained in two independent experiments also performed in triplicate.

imental Procedures." Nanomolar RTX and micromolar ANA induced Ca^{2+} uptake at both high and low pH, although with different characteristics. At pH 5.5 ANA was a full agonist of VR1 and produced maximal transport comparable with nanomolar concentrations of RTX. At pH 7.5, RTX exhibited a lower affinity but produced a much higher maximal Ca^{2+} uptake. ANA at this pH, even at a 70 μ M concentration, had very low affinity and capacity. These data suggest that VR1 can be protonated and that protonation substantially alters the channel function of VR1. Nontransfected NIH 3T3 cells did not respond to these ligands or acidification of the medium.

The activity of other eicosanoids with structural similarity to ANA and the ability of CPZ to antagonize their activity were examined using Ca^{2+} uptake experiments in primary DRG cultures. The rank order of activity of four eicosanoids was 12(S)HPTE > PGD₂ > PGE₂, with 12(S)HETE being inactive. Like ANA, these compounds activated $^{45}Ca^{2+}$ uptake in the micromolar range (5 μ M each in this experiment). For each active eicosanoid, the induced $^{45}Ca^{2+}$ uptake was completely inhibited by co-treatment with 10 μ M CPZ, indicating the vanilloid receptor specificity of the uptake (Fig. 4).

The direct binding of [³H]ANA to VR1 was investigated in

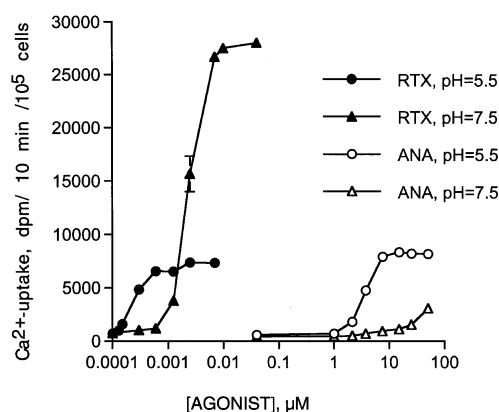


FIG. 3. H^+ dependence of ANA- and RTX-induced VR1-mediated Ca^{2+} uptake. NIH 3T3 cells stably expressing VR1 ϵ were seeded in 24-well plates 1 day before the experiment. Ca^{2+} uptake assays were carried out in buffer adjusted to pH 5.5 and 7.5, as indicated. At pH 5.5 both ligands induced a VR1-mediated high affinity and low capacity form of Ca^{2+} uptake. At neutral pH, RTX has a lower affinity but induces a much higher capacity Ca^{2+} uptake, whereas ANA was nearly ineffective. Each experiment was repeated at least two additional times in triplicate with similar results.

ectopic expression systems. In addition to the CB1 and CB2 cannabinoid-binding sites, a high capacity transporter and a coupled metabolic enzyme, which hydrolyzes intracellularly accumulated ANA to arachidonic acid and ethanolamine, have recently been reported to be present in a wide spectrum of cells (37, 38). To prevent transport and metabolic effects, [³H]ANA binding was performed at 4 $^{\circ}$ C in intact, nontransfected HEK293 and COS7 cells and after transient expression of VR1eGFP. Even nontransfected HEK293 cells, kept on ice, were able to bind and/or accumulate [³H]ANA, and this could be competed with 70 μ M nonlabeled ANA (Fig. 5a). This transport/metabolic process was insensitive to competition by either RTX (1 or 10 nM), CAP (1 or 10 μ M), or CPZ (1 or 10 μ M). Only OLV, an analog of both vanilloids and cannabinoids produced an inhibition of [³H]ANA binding: no competition at 7 μ M and partial competition at 70 μ M (not shown). The latter data suggest that the transport/metabolic process of these cells is capable of interacting specifically with ANA even at 4 $^{\circ}$ C but not with vanilloids.

When VR1eGFP was transiently expressed, [³H]ANA binding was augmented about 2–3-fold above the nontransfected control (first bar in Fig. 5a), demonstrating the interaction of ANA with VR1 (Fig. 5b). Co-incubation of 70 μ M nonlabeled ANA, as well as 1 or 10 nM RTX, 1 or 10 μ M CAP, and 0.5 μ M OLV displaced 54, 18, 38, 9, 27, and 32% of [³H]ANA, respectively. Displacement of [³H]ANA either with vanilloids or ANA strongly supports the view that ANA binds to VR1, whereas the inability of vanilloids to interfere with ANA at the cannabinoid transport/metabolic system distinguishes it from VR1 (Fig. 5 legend).

The experiments above demonstrated that ANA can induce Ca^{2+} uptake at acidic conditions (pH \leq 6.5) in DRG neurons and in cells ectopically expressing VR1 recombinants. To address the effects of ANA and pH on intracellular free Ca^{2+} ($[Ca^{2+}]_i$), DRG neurons were subjected to double wavelength fluorescent ratio imaging at pH 6.0. DRG neurons were selected by their Indo-1 fluorescence, and regions of interest were marked over the perikarya for ratiometric imaging. Typical results are shown after treatment with ANA (35 μ M) in Fig. 6. The ratio of fluorescence at (405/485 nm) was increased (average of three of the small size neurons in the field of view), indicative of ANA-induced accumulation of Ca^{2+} . In contrast, larger size neurons in the same field of

FIG. 4. **Effect of eicosanoids, 12(S)HPTE, PGD₂, PGE₂, and 12(S)HETE, on $^{45}\text{Ca}^{2+}$ uptake of DRG cultures.** Different eicosanoids were applied in 5 μM concentration for 10 min at 34 °C in the $^{45}\text{Ca}^{2+}$ -assay medium (HCB, pH 6.0). All eicosanoids except 12(S)HETE induced significant $^{45}\text{Ca}^{2+}$ uptake in DRG cultures. To show vanilloid specific activity of eicosanoids, 10 μM CPZ was co-incubated with the drugs as indicated. CPZ almost completely blocked the eicosanoid-induced Ca^{2+} transport, indicating VR1 specificity. Each point represents the mean \pm S.E. of triplicate determinations. Similar results were obtained in two independent experiments performed in triplicate.

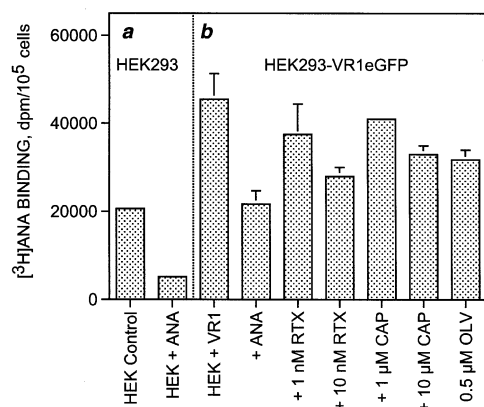
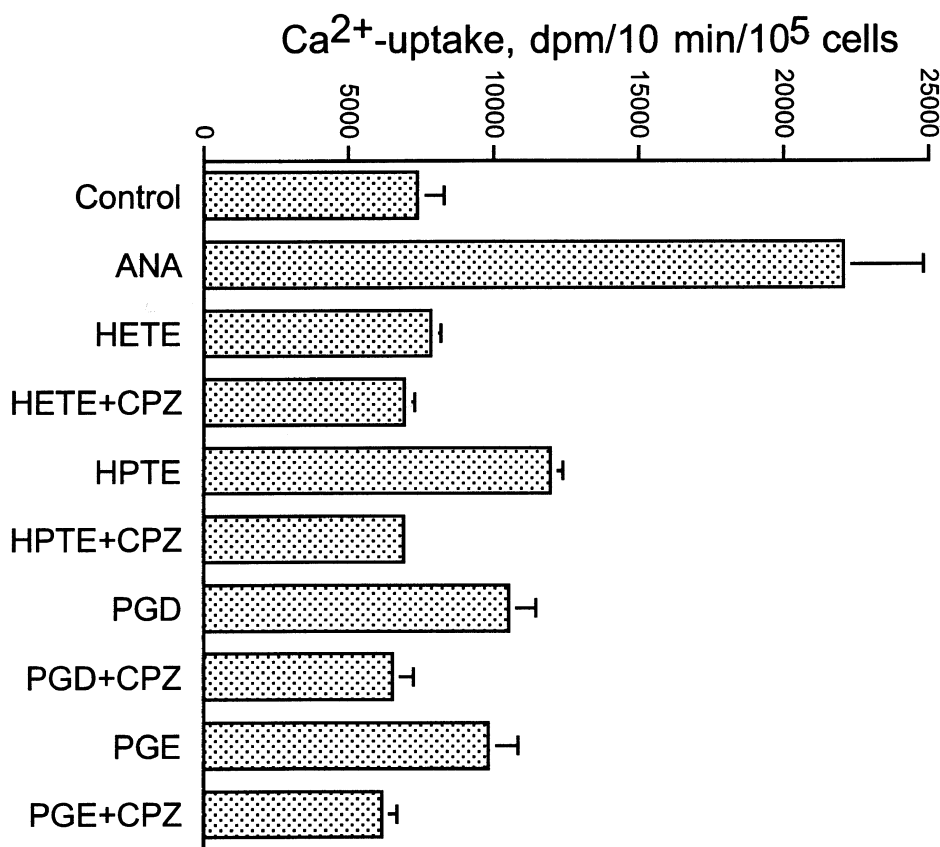


FIG. 5. **[^3H]ANA binding in live nontransfected HEK293 line (a) and HEK293 cells transiently expressing VR1eGFP (b).** The binding assays were performed in intact cells kept on ice for 40 min in calcium-free medium (see "Experimental Procedures"). To analyze the specificity of binding 70 μM nonlabeled ANA, 1 or 10 nM RTX and 1 μM CAP were co-incubated in the assay as indicated. *a*, nontransfected HEK293 cells at 4 °C bound/transported [^3H]ANA, which could be competed with 70 μM nonlabeled ANA. The transport/metabolic process for ANA was insensitive to competition by RTX (1 or 10 nM), CAP (1 or 10 μM), CPZ (1 or 10 μM), or OLV (7 μM) (not shown, see "Results"). *b*, expression of VR1eGFP more than doubled [^3H]ANA binding. Different vanilloid ligands competed with [^3H]ANA, as indicated. Each bar represents the mean \pm S.E. of triplicate determinations. Similar results were obtained in three independent experiments performed in triplicate.

view showed no change in fluorescence ratio over time and no response upon addition of ANA.

Subramanian and Meyer demonstrated that elevation of $[\text{Ca}^{2+}]_i$ with either the Ca^{2+} ionophore, ionomycin, or thapsigargin, an inhibitor of the SERCA ATPase involved in reuptake of Ca^{2+} to the ER, caused fragmentation of the ER (32). We utilized this fragmentation effect in a previous report examin-

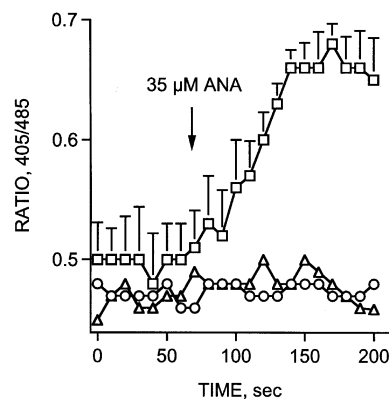


FIG. 6. **ANA induced accumulation of $[\text{Ca}^{2+}]_i$ determined by ratiometric imaging of DRG neurons.** Individual DRG neurons were selected, and their perikarya were marked for ratiometric imaging in the field of a 40 \times objective. Following base-line recording, 100 μl of ANA was added to make a 35 μM final concentration in the HCB medium (pH 6.0), at the indicated time point. The ratio of emitted fluorescence intensity at 405 and 485 was calculated simultaneously from selected large ($\sim 1000 \mu\text{m}^2$) and small size ($\sim 250 \mu\text{m}^2$) neurons; the latter population contains the C-fiber nociceptors, which express VR1. The data shown are from a field of view containing five neurons. The curve showing the increase in ratio is from three small size neurons exhibiting a Ca^{2+} response (symbols represent the means of emitted fluorescence ratio \pm S.E.). The lower curves are recordings from the two large size neurons that did not show an elevation in fluorescence ratio.

ing vanilloid-induced Ca^{2+} influx, and it provides a robust end point for optically based determinations of VR1 agonist activity. We also demonstrated that the normally filamentous mitochondria undergo vesiculation concurrently with the ER upon abrupt elevation of $[\text{Ca}^{2+}]_i$ (35). These ligand-activated processes were examined in cultures expressing VR1eGFP (green) preloaded with the MitoTracker dye (red), which is a vital fluorescent marker of mitochondria. The cells were then imaged by dual wavelength fluorescent confocal microscopy. In

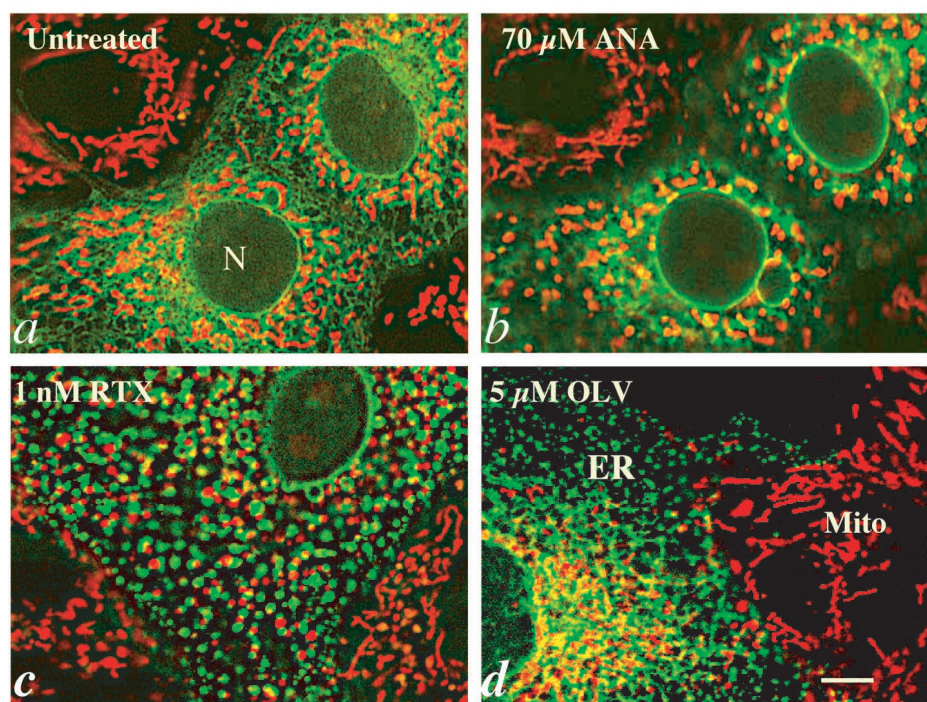


FIG. 7. Intracellular remodeling after treatment with RTX, OLV, or ANA in live COS7 cells expressing VR1eGFP. Double fluorescence labeling and confocal microscopy were employed to examine agonist activity *via* early intracellular membrane changes. The cells were labeled *in vivo* by incubation with $0.5\ \mu\text{M}$ MitoTracker for 30 min. MitoTracker (red) and VR1eGFP (green) fluorescence were recorded simultaneously by dual wavelength confocal imaging. To demonstrate remodeling of cell organelles after treatments with agonists, green VR1GFP labeling of intracellular membranes was usurped. In *panel a*, four COS7 cells are shown before treatment with agonist. Two of them are nontransfected (red only), and the other two are expressing VR1eGFP showing both green and red fluorescence. The morphological transformation of the ER and mitochondria (Mito) are depicted 30 s after $70\ \mu\text{M}$ ANA administration (*panel b*). In two additional cultures with the same organelle labeling, $1\ \text{nM}$ RTX (*panel c*) and $5\ \mu\text{M}$ OLV (*panel d*) treatment produced similar fragmentation of the ER and mitochondria. No such remodeling of the mitochondria (and by inference the ER) occurred in adjacent nontransfected cells (red only). Similar changes were noted in two independent experiments carried out either with HEK293 or COS7 cell lines. Scale bar, $5\ \mu\text{m}$.

addition to functioning at the plasma membrane as a Ca^{2+} ionophore (Figs. 1–4), VR1eGFP is also present in the ER in COS7 (Fig. 7a), HEK293, and NIH 3T3 cells (35). This localization provides the fluorescent label for the ER compartment in the present experiments, which were done in COS7 cells (Fig. 7).

Application of $1\ \text{nM}$ RTX, $5\ \mu\text{M}$ OLV, and $70\ \mu\text{M}$ ANA induced a rapid ($<30\ \text{s}$) fragmentation of the intracellular membranes. The effect was similar with ANA, OLV, or RTX. Changes included transformation of the ER network into vesicles and rounding up of the mitochondria. Additional hallmarks of Ca^{2+} cytotoxicity were observed, such as nuclear envelope blebbing (Fig. 7, *b*, *c*, and *d* versus *a*) and rounding up the cells after $\sim 1\ \text{h}$ (not shown, illustrated in Ref. 35). None of these drug effects were noted in adjacent nontransfected cells, which are only stained red with the MitoTracker dye (Fig. 7a). The intracellular fragmentation was only seen upon agonist treatment in VR1-transfected cells. At least five experiments were performed with each drug, and *all* VR1eGFP-positive cells that we observed underwent ER and mitochondrial remodeling. These data strongly suggest that sensitivity to vanilloids and eicosanoids was solely conferred by ectopic expression of VR1 in the heterologous cells.

To simulate tissue acidification, cells were cultured in complete DMEM in the absence of HEPES buffer for 24 h. Under these conditions the pH gradually drops to 6.0 ± 0.5 , determined in repeated experiments, and the DRG cultures were incubated for additional 24 h in the presence of $25\ \text{nM}$ RTX, $50\ \mu\text{M}$ OLV or $70\ \mu\text{M}$ ANA. Western blot analysis in Fig. 8 shows a typical result of these treatments. All three drugs substantially reduced VR1 immunoreactivity compared with untreated cells. The blots, prepared from the primary DRG cultures, were

stripped and reprobed with an anti-cytochrome *c* antibody (Fig. 8a, *Cyt. c*). Densitometric scans demonstrated little or any decrease in the cytochrome *c* levels despite the fact that the cultures exhibited 99, 74, and 75% losses of VR1-specific immunoreactivity after OLV, RTX, and ANA treatment, respectively (Fig. 8b). Withdrawal of HEPES buffer from the DRG culture medium for 48 h did not significantly reduce either the levels of VR1 or cytochrome *c* of nontreated cells (not shown). The selective loss suggests that vanilloid agonists and ANA effectively removed the subpopulation of VR1-positive cells from the primary cultures, a result consistent with the imaging studies performed in VR1eGFP-expressing cells (Fig. 7).

DISCUSSION

The present report provides evidence that eicosanoids, particularly the endocannabinoid, anandamide, bind to VR1 and activate Ca^{2+} uptake in specific DRG neurons in a pH-dependent manner. Small size neurons in the DRG uniquely express VR1, which is also known to be sensitive to acidification of the extracellular milieu (6–8, 10). To date the vanilloid-agonist activity of ANA (*i.e.* actions antagonized by CPZ) has been demonstrated only in a vasodilatation model in animals (17, 39). The direct [^3H]ANA binding studies on VR1-expressing cells extend these observations and provide evidence that ANA, in addition to the CB1 and CB2 receptors, binds to VR1 and is displaced with vanilloid compounds. We demonstrate that ANA binding to VR1 activates Ca^{2+} transport in a pH-dependent fashion in dissociated DRG neuron cultures and in cells ectopically expressing VR1 (Fig. 1). By themselves, neither the DRG cultures nor the VR1-expressing cell lines responded to acidification of the milieu with Ca^{2+} uptake. Likewise, vanilloids and CPZ had no effect on nontransfected cells. However, CPZ

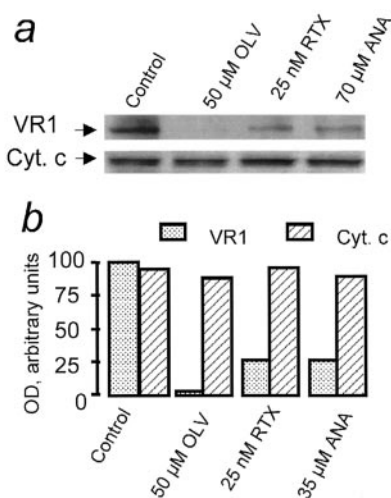


FIG. 8. Western blot analysis of DRG cultures treated with vanilloids and ANA. DRG cultures were prepared as described under "Experimental Procedures" and plated in complete DMEM containing 20 mM HEPES (pH 7.4) in 24-well plates. After 2 days, cells were changed into complete DMEM prepared without HEPES buffer and cultured for an additional 24 h. After 24 h the pH levels of the supernatants of the cultures were determined to be 6.1 ± 0.4 , and then 25 nM RTX, 50 μ M OLV, or 70 μ M ANA was added. After 24 h DRG cultures were harvested in 50 μ l denaturing SDS lysis buffer. Total protein extracts (15 μ g from each sample) were analyzed by Western blotting. The blots were probed first with an affinity-purified antibody raised against the first 18 amino acids of rat VR1. The immunoreactive bands were visualized by enhanced chemiluminescence on x-ray film. The top arrow points toward the immunoreactive 93-kDa band specific to VR1. All three drugs substantially reduced VR1 immunoreactivity compared with control DRG cultures (panel a, upper section). To demonstrate equal protein loading, the same blot was stripped and reprobed with a cytochrome *c*-specific (Cyt. *c*) antiserum (panel a, lower section). VR1 and cytochrome *c* specific bands were scanned, and the optical density (OD) was quantitated by the NIH Image software (panel b). The data presented are from the same batch of DRG cultures distributed in a 24-well plate for different treatments. Similar results were obtained from two additional batches of DRG cultures analyzed in duplicate.

inhibited Ca^{2+} uptake in DRG neuron cultures or the VR1-expressing cell systems when co-incubated with either vanilloids or ANA (Fig. 2). Our data also suggest that a pH of ≤ 6.5 can change VR1 into a conformation distinct from that at pH 7.5. The acidic conformation promotes ANA-induced Ca^{2+} uptake in VR1-expressing cells (Fig. 3). A previous work studied ANA activation of human VR1-mediated Ca^{2+} uptake at pH 6.4 and 7.4 and consequently was only able to employ heterologous expression systems (28). The present evidence demonstrates that acidification potentiates the activity of ANA and perhaps other eicosanoids at rat VR1. In addition to ANA, products of lipoxygenases, including endogenous capsaicin-like substances such as 12- and 15-(S)- hydroperoxyeicosatetraenoic acids, 5- and 15-(S)- hydroxyeicosatetraenoic acids, and leukotriene B (4), also activate VR1 expressed in HEK293 cells (4) using electrophysiological methods, a result we extend with Ca^{2+} uptake and [3H]ANA binding. Taken together, the data in this paper and recent observations support the view that certain products of lipoxygenases and ANA under acidic conditions can serve as endogenous ligands of VR1. The combined effect of high eicosanoid release and low pH might contribute to pain signaling to the CNS *in vivo*.

Previously, acidification was noted to sensitize nociceptive neurons toward vanilloids (40, 41) and eicosanoids including, but probably not confined to, PGE_2 and prostacyclin (18, 20, 21, 42, 43). In addition to acid-sensitive sodium ion channels (44–46), recent point mutation studies implicate H^+ as a direct regulator of VR1. Acidification of the extracellular medium apparently exerts its effects on the Glu⁶⁰⁰ residue located in the

pore loop region of VR1. This region may be distinct from the putative binding site(s) of lipid ligands, which remains to be elucidated (10). Here we provide further evidence that an acidic environment dramatically changes the affinity and transport kinetics of VR1 in transfected cells or DRG neurons (Figs. 1–3). The kinetic parameters of ligand-induced activation in Fig. 3 suggest that association/dissociation of H^+ with VR1 at the cell surface changes VR1 into high and low affinity forms, respectively. Low pH promotes while neutral pH inhibits the efficacy of ANA to activate VR1 (Fig. 3; high affinity Ca^{2+} uptake with low V_{max} , at pH 5.5 and vice versa at 7.5).

In addition to Ca^{2+} transport, the binding data with [3H]ANA demonstrate that ANA directly interacts with VR1 in living cells. Although vanilloids can displace [3H]ANA at binding site(s) on VR1, they apparently do not affect transmembrane transport of this eicosanoid (see "Results" and Fig. 5 legend). ANA and potentially other eicosanoids (4) released in disease states (47) coincidentally with tissue acidification can serve as activators of VR1 (17, 48, 49). The potent blockade of eicosanoid-induced Ca^{2+} uptake by CPZ determined here and observations made earlier (4, 17) imply that inflammatory metabolites of the lipoxygenase and cyclooxygenase pathways might activate VR1 *in vivo*.

Transmembrane transport of ANA was reported in different cell types including neurons, astrocytes, and liver cells (37, 50, 51). An intracellular hydrolase, tightly coupled to the transporter, which splits ANA to arachidonic acid and ethanolamine, was characterized in a wide variety of cells (37, 38). Through heterologous expression of VR1, we were able to differentiate between ANA transport/metabolism and ANA binding to VR1 as well as its ability to functionally elicit specific Ca^{2+} uptake.

The ratio imaging of ANA-induced increases in $[Ca^{2+}]_i$ in DRG neurons clearly showed specific stimulation of VR1 ionophore activity, which corroborates the observations of others employing electrophysiological techniques (17, 18). Ca^{2+} -induced transient disruption of ER can occur under conditions of physiological stimulation, such as reported for fertilization of oocytes (52). Here we show that ANA, like vanilloids (35), promotes rapid intracellular membrane remodeling of the ER and morphological transformation of mitochondria (Fig. 7). These changes can lead to cell death, whereas at injury sites remote from the cell body, such processes may damage VR1-positive axons or nerve terminals. To avoid cytotoxicity, even under less extreme situations *in vivo*, VR1-positive nociceptors probably are endowed with precise regulation of $[Ca^{2+}]_i$ (53–55), including high capacity scavenger functions of mitochondria (56, 57), although *in vivo*, eicosanoids seems to affect only the protonated form of VR1, which likely confines these actions to inflamed or ischemic tissues. Protonated VR1 may start to react to $\leq 1 \mu$ M concentrations of eicosanoids or to particular mixtures of these substances (*i.e.* "inflammatory soup") (58). PGE_2 was reported to potentiate the effects of suboptimal concentrations of CAP (48, 49). It is also conceivable that in pathological situations eicosanoids may temporally reach micromolar levels, as observed (59). ANA in that concentration probably is effective not only on conventional receptors such as CB1 or CB2 but on VR1 presented by C-type fibers of polymodal nociceptors all over the body, including the skin and internal organs. In fact, it is known that inflammatory conditions can recruit populations of "silent nociceptors," which are only active in the presence of inflammatory mediators (60).

In summary, ANA and other eicosanoids can interact with VR1 in a fashion similar to vanilloids, although with much lower affinity. [3H]ANA binds to VR1 expressed in heterologous cell systems and is displaced by vanilloids, suggesting competitive interaction with VR1. The data in this paper implicate

endogenous arachidonic acid derivatives, including ANA, as conditional, endogenous ligands of vanilloid receptor(s). Eicosanoids and H^+ , overproduced in pathological situations potentiate each other to trigger VR1 exposed on nociceptive neurons. Eicosanoids and protons released by noxious heat, mechanical, and ischemic injury as well as inflammation may stimulate pain transmission through this mechanism.

REFERENCES

- Edgemond, W. S., Hillard, C. J., Falck, J. R., Kearn, C. S., and Campbell, W. B. (1998) *Mol. Pharmacol.* **54**, 180–188
- Marriott, D., Wilkin, G. P., Coote, P. R., and Wood, J. N. (1991) *Adv. Prostaglandin Thromboxane Leukotriene Res.* **21**, 739–741
- Dirig, D. M., and Yaksh, T. L. (1999) *Br. J. Pharmacol.* **126**, 1333–1340
- Hwang, S. W., Cho, H., Kwak, J., Lee, S. Y., Kang, C. J., Jung, J., Cho, S., Min, K. H., Suh, Y. G., Kim, D., and Oh, U. (2000) *Proc. Natl. Acad. Sci. U. S. A.* **97**, 6155–6160
- Stevens, C. R., Williams, R. B., Farrell, A. J., and Blake, D. R. (1991) *Ann. Rheum. Dis.* **50**, 124–132
- Bevan, S., and Geppetti, P. (1994) *Trends Neurosci.* **17**, 509–512
- Caterina, M. J., Schumacher, M. A., Tominaga, M., Rosen, T. A., Levine, J. D., and Julius, D. (1997) *Nature* **389**, 816–824
- Tominaga, M., Caterina, M. J., Malmberg, A. B., Rosen, T. A., Gilbert, H., Skinner, K., Raumann, B. E., Basbaum, A. I., and Julius, D. (1998) *Neuron* **21**, 531–543
- Caterina, M. J., Rosen, T. A., Tominaga, M., Brake, A. J., and Julius, D. (1999) *Nature* **398**, 436–441
- Jordt, S. E., Tominaga, M., and Julius, D. (2000) *Proc. Natl. Acad. Sci. U. S. A.* **97**, 8134–8139
- Welch, J. M., Simon, S. A., and Reinhart, P. H. (2000) *Proc. Natl. Acad. Sci. U. S. A.* **97**, 13889–13894
- Baumann, T. K., and Martenson, M. E. (2000) *J. Neurosci.* **20**, 80
- Jung, J., Hwang, S. W., Kwak, J., Lee, S. Y., Kang, C. J., Kim, W. B., Kim, D., and Oh, U. (1999) *J. Neurosci.* **19**, 529–538
- Dux, M., Sann, H., Schemann, M., and Jancso, G. (1999) *Cell Tissue Res.* **296**, 471–477
- Kwak, J. Y., Jung, J. Y., Hwang, S. W., Lee, W. T., and Oh, U. (1998) *Neuroscience* **86**, 619–626
- Stern, O., and Szallasi, A. (1999) *Trends Pharmacol. Sci.* **20**, 459–465
- Zygmunt, P. M., Petersson, J., Andersson, D. A., Chuang, H., Sorgard, M., Di Marzo, V., Julius, D., and Hogestatt, E. D. (1999) *Nature* **400**, 452–457
- Vyklicky, L., Knotkova-Urbancova, H., Vitaskova, Z., Vlachova, V., Kress, M., and Reeh, P. W. (1998) *J. Neurophysiol.* **79**, 670–676
- Melck, D., Bisogno, T., De Petrocellis, L., Chuang, H., Julius, D., Bifulco, M., and Di Marzo, V. (1999) *Biochem. Biophys. Res. Commun.* **262**, 275–284
- Robertson, J. T., Huffmon, G. V., III, Thomas, L. B., Leffler, C. W., Gunter, B. C., and White, R. P. (1996) *Spine* **21**, 1731–1736
- Noda, K., Ueda, Y., Suzuki, K., and Yoda, K. (1997) *Brain Res.* **751**, 348–351
- Richardson, J. D., Kilo, S., and Hargreaves, K. M. (1998) *Pain* **75**, 111–119
- Zimmer, A., Zimmer, A. M., Hohmann, A. G., Herkenham, M., and Bonner, T. I. (1999) *Proc. Natl. Acad. Sci. U. S. A.* **96**, 5780–5785
- Jaggard, S. I., Hasnie, F. S., Sellaturay, S., and Rice, A. S. (1998) *Pain* **76**, 189–199
- Costa, B., Vailati, S., and Colleoni, M. (1999) *Behav. Pharmacol.* **10**, 327–331
- Martin, W. J., Loo, C. M., and Basbaum, A. I. (1999) *Pain* **82**, 199–205
- Jerman, J. C., Brough, S. J., Prinjala, R., Harries, M. H., Davis, J. B., and Smart, D. (2000) *Br. J. Pharmacol.* **130**, 916–922
- Smart, D., Gunthorpe, M. J., Jerman, J. C., Nasir, S., Gray, J., Muir, A. I., Chambers, J. K., Randall, A. D., and Davis, J. B. (2000) *Br. J. Pharmacol.* **129**, 227–230
- Smart, D., and Jerman, J. C. (2000) *Trends Pharmacol. Sci.* **21**, 134
- Szolcsanyi, J. (2000) *Trends Pharmacol. Sci.* **21**, 41–42
- Zygmunt, P. M., Julius, D., Di Marzo, V., and Hogestatt, E. D. (2000) *Trends Pharmacol. Sci.* **21**, 43–44
- Subramanian, K., and Meyer, T. (1997) *Cell* **89**, 963–971
- Grimaldi, M., Favitt, A., and Alkon, D. L. (1999) *J. Biol. Chem.* **274**, 33557–33564
- Pedrosa Ribeiro, C. M., McKay, R. R., Hosoki, E., Bird, G. S., and Putney, J. W., Jr. (2000) *Cell Calcium* **27**, 175–185
- Olah, Z., Szabo, T., Karai, L., Hough, C., Fields, R. D., Caudle, R. M., Blumberg, P. M., and Iadarola, M. J. (2000) *J. Biol. Chem.* **276**, 11021–11030
- Olah, Z., Lehel, C., Jakab, G., and Anderson, W. B. (1994) *Anal. Biochem.* **221**, 94–102
- Beltramo, M., Stella, N., Calignano, A., Lin, S. Y., Makriyannis, A., and Piomelli, D. (1997) *Science* **277**, 1094–1097
- Cravatt, B. F., Giang, D. K., Mayfield, S. P., Boger, D. L., Lerner, R. A., and Gilula, N. B. (1996) *Nature* **384**, 83–87
- Ralevic, V., Kendall, D. A., Randall, M. D., Zygmunt, P. M., Movahed, P., and Hogestatt, E. D. (2000) *Br. J. Pharmacol.* **130**, 1483–1488
- Petersen, M., and LaMotte, R. H. (1993) *Pain* **54**, 37–42
- Kress, M., Fetzter, S., Reeh, P. W., and Vyklicky, L. (1996) *Neurosci. Lett.* **211**, 5–8
- Murata, T., Ushikubi, F., Matsuoka, T., Hirata, M., Yamasaki, A., Sugimoto, Y., Ichikawa, A., Aze, Y., Tanaka, T., Yoshida, N., Ueno, A., Oh-ishi, S., and Narumiya, S. (1997) *Nature* **388**, 678–682
- Ballou, L. R., Botting, R. M., Goorha, S., Zhang, J., and Vane, J. R. (2000) *Proc. Natl. Acad. Sci. U. S. A.* **97**, 10272–10276
- Waldmann, R., Bassilana, F., de Weille, J., Champigny, G., Heurteaux, C., and Lazdunski, M. (1997) *J. Biol. Chem.* **272**, 20975–20978
- Bassilana, F., Champigny, G., Waldmann, R., de Weille, J. R., Heurteaux, C., and Lazdunski, M. (1997) *J. Biol. Chem.* **272**, 28819–28822
- Waldmann, R., Champigny, G., Bassilana, F., Heurteaux, C., and Lazdunski, M. (1997) *Nature* **386**, 173–177
- Calignano, A., Katona, I., Desarnaud, F., Giuffrida, A., La Rana, G., Mackie, K., Freund, T. F., and Piomelli, D. (2000) *Nature* **408**, 96–101
- Lopshire, J. C., and Nicol, G. D. (1998) *J. Neurosci.* **18**, 6081–6092
- Lopshire, J. C., and Nicol, G. D. (1997) *J. Neurophysiol.* **78**, 3154–3164
- Di Marzo, V., Bisogno, T., Melck, D., Ross, R., Brockie, H., Stevenson, L., Pertwee, R., and De Petrocellis, L. (1998) *FEBS Lett.* **436**, 449–454
- Beltramo, M., and Piomelli, D. (1999) *Eur. J. Pharmacol.* **364**, 75–78
- Terasaki, M., Jaffe, L. A., Hunnicutt, G. R., and Hammer, J. A., III (1996) *Dev. Biol.* **179**, 320–328
- Choi, D. W. (1988) *Trends Neurosci.* **11**, 465–469
- Yu, S. P., Yeh, C., Strasser, U., Tian, M., and Choi, D. W. (1999) *Science* **284**, 336–339
- Berridge, M. J. (1998) *Neuron* **21**, 13–26
- Simpson, P. B., and Russell, J. T. (1998) *Brain Res. Rev.* **26**, 72–81
- Dedov, V. N., and Roufogalis, B. D. (2000) *Neuroscience* **95**, 183–188
- Kessler, W., Kirchhoff, C., Reeh, P. W., and Handwerker, H. O. (1992) *Exp. Brain Res.* **91**, 467–476
- Piomelli, D., Giuffrida, A., Calignano, A., and Rodriguez de Fonseca, F. (2000) *Trends Pharmacol. Sci.* **21**, 218–224
- Lynn, B. (1991) *Trends Neurosci.* **14**, 95